Published in final edited form as:
Neuron. 2014 December 3; 84(5): 919–926. doi:10.1016/j.neuron.2014.10.046.

CaMKI-dependent regulation of sensory gene expression mediates experience-dependent plasticity in the operating range of a thermosensory neuron

Yanxun V. Yu[#1], **Harold W. Bell**[#1], **Dominique Glauser**[3], **Stephen D. Van Hooser**[4], **Miriam B. Goodman**[5], and **Piali Sengupta**[1,6]

[1]Department of Biology, National Center for Behavioral Genomics Brandeis University Waltham, MA 02454 [3]Department of Biology University of Fribourg Fribourg 1700, Switzerland [4]Department of Biology, National Center for Behavioral Genomics Brandeis University Waltham, MA 02454 [5]Department of Molecular and Cellular Physiology Stanford University School of Medicine Palo Alto, CA 94305

[#] These authors contributed equally to this work.

SUMMARY

Sensory adaptation represents a form of experience-dependent plasticity that allows neurons to retain high sensitivity over a broad dynamic range. The mechanisms by which sensory neuron responses are altered on different timescales during adaptation are unclear. The threshold for temperature-evoked activity in the AFD thermosensory neurons (T^*_{AFD}) in *C. elegans* is set by the cultivation temperature (T_c), and regulated by intracellular cGMP levels. We find that T^*_{AFD} adapts on both short and long timescales upon exposure to temperatures warmer than T_c, and that prolonged exposure to warmer temperatures alters expression of AFD-specific receptor guanylyl cyclase genes. These temperature-regulated changes in gene expression are mediated by the CMK-1 CaMKI enzyme which exhibits T_c-dependent nucleocytoplasmic shuttling in AFD. Our results indicate that CaMKI-mediated changes in sensory gene expression contribute to long-term adaptation of T^*_{AFD}, and suggest that similar temporally and mechanistically distinct phases may regulate the operating ranges of other sensory neurons.

INTRODUCTION

Animals continuously modulate their behavior as a function of current and past experience. Sensory adaptation is a well-studied form of experience-dependent behavioral plasticity that occurs on a range of timescales. Adaptation to prevailing environmental cues resets the behavioral response threshold and regulates gain, thereby allowing animals to maintain sensitivity to sensory signals over a broad dynamic range. On short timescales, desensitization of sensory neuron responses to external cues can arise from altered trafficking or functions of primary sensory signal transduction molecules (eg. Kurahashi and Menini, 1997; Sokolov et al., 2002). Although sensory adaptation on long timescales of

[6]Corresponding author: sengupta@brandeis.edu; 781-736-2686 (Ph).

hours to days has also been reported (Bao and Engel, 2012; Dalton and Wysocki, 1996), the mechanisms underlying long-term adaptation remain poorly described. A few reports to date have suggested that altered sensory gene expression or protein turnover can contribute to long-term desensitization of peripheral sensory neuron responses and behavioral acclimation (Juang et al., 2013; Patapoutian et al., 2009; Zhang et al., 2013), but whether similar mechanisms operate more broadly has not been fully established.

Thermosensation in *C. elegans* provides an excellent system in which to study the neuronal and molecular mechanisms underlying experience-dependent sensory adaptation. In the physiological temperature range of 15°-25°C, *C. elegans* acclimates to its cultivation temperature (T_c) and exhibits distinct thermotactic navigation behaviors in temperature ranges relative to T_c (Hedgecock and Russell, 1975) (Figure 1A). At temperatures (T) above T_c, animals robustly move towards colder temperatures (negative thermotaxis), whereas at $T \sim T_c$, animals track isotherms (isothermal tracking or IT behavior) (Garrity et al., 2010; Hedgecock and Russell, 1975; Mori and Ohshima, 1995) (Figure 1A). Under a circumscribed set of conditions at $T < T_c$, animals exhibit positive thermotaxis, but are otherwise athermotactic (Jurado et al., 2010; Ramot et al., 2008b) (Figure 1A). Computational models suggest that this experience-dependent behavioral plasticity may allow *C. elegans* to maximize fitness over its physiological temperature range in its natural habitats (Ramot et al., 2008b).

Behavioral acclimation to T_c is mediated in part via adaptation of the temperature response threshold (T^*_{AFD}) of the bilateral AFD neuron pair, the primary thermosensory neuron type in *C. elegans* (Clark et al., 2006; Kimura et al., 2004; Ramot et al., 2008a). T_c regulates T^*_{AFD}, and responses to temperature changes are detected in AFD only at $T > T^*_{AFD}$. Although the molecular thermosensor(s) in AFD are unknown, the second messenger cGMP is required for thermotransduction, as well as for setting the appropriate T^*_{AFD} (reviewed in Garrity et al., 2010). Upon warming, cGMP levels are thought to increase due to increased cGMP synthesis, decreased cGMP degradation, or both. T^*_{AFD} is thus defined as the lowest temperature at which the net increase in intracellular cGMP levels leads to opening of cGMP-gated channels and depolarization. Adaptation of T^*_{AFD} to a new temperature may involve feedback that subsequently resets cGMP concentrations to resting levels. The mechanisms by which cGMP levels are altered as a function of exposure to new temperatures to regulate T^*_{AFD}, and thus the operating range of AFD, are unclear.

Here we show that the CMK-1 calcium/calmodulin-dependent protein kinase I (CaMKI) plays a critical role in adaptation of T^*_{AFD} to T_c. Through detailed analysis of the time-dependence of T^*_{AFD} adaptation to warmer temperatures, we demonstrate that the process has both fast and slow components occurring on timescales of minutes and hours, respectively. We also show that the expression of AFD-specific *gcy* receptor guanylyl cyclase (rGC) genes implicated in cGMP synthesis and T^*_{AFD} setting is altered in a T_c- and CMK-1-dependent manner upon prolonged exposure to a new temperature. Moreover, correct adaptation of T^*_{AFD} requires T_c-dependent regulation of CMK-1 subcellular localization in AFD. Our observations suggest that CMK-1-mediated changes in the expression of sensory signaling genes are a major determinant of long-term plasticity in the

operating range of AFD, and suggest that similar mechanisms may operate to fine-tune the responsiveness of other sensory neurons.

RESULTS

Multifunctional calcium/calmodulin-binding proteins such as CaMKI and CaMKIV link intracellular calcium dynamics with changes in neuronal development and function (Wayman et al., 2008). *cmk-1* encodes the sole CaMKI/IV ortholog in *C. elegans* (Eto et al., 1999), and we previously showed that *cmk-1* mutants exhibit defects in negative thermotaxis behavior (Satterlee et al., 2004). Since multiple thermosensory neurons contribute to negative thermotaxis behaviors in *C. elegans* (Beverly et al., 2011), we re-examined negative thermotaxis behavioral phenotypes of *cmk-1* mutants under conditions that specifically require AFD function (Beverly et al., 2011). AFD is also required for positive thermotaxis under a limited set of conditions (Jurado et al., 2010; Luo et al., 2014); this behavior was not further examined here.

Worms perform negative thermotaxis using a biased random walk strategy (Garrity et al., 2010). This navigation strategy can be quantified by calculating the thermotaxis bias defined as the [(total duration of movement or runs toward warmer temperatures) – (total duration of runs toward colder temperatures)]/total run duration. Although animals use a reorientation strategy that increases the probability of orienting new runs towards colder temperatures (Luo et al., 2014), we did not measure reorientation in these assays. Under conditions known to require AFD for negative thermotaxis (Beverly et al., 2011; see Supplemental Experimental Procedures), *cmk-1(oy21)* putative null and *cmk-1(oy20)* missense mutants exhibited strong defects in negative thermotaxis behavior on spatial thermal gradients (Figure 1B). This behavioral defect was rescued by expressing wild-type *cmk-1* sequences specifically in AFD, but not in the AWC, thermosensory neurons (Figure 1B).

Animals mutant for *cmk-1* were also examined for their ability to track isotherms, an AFD-dependent behavior (Mori and Ohshima, 1995). We quantified track numbers to measure initiation of tracking, as well as track lengths to measure maintenance of tracking behavior. *cmk-1* mutant strains were strongly defective in track initiation, and weakly defective in track maintenance, regardless of T_c (Figure 1C-D). IT behaviors at all examined temperatures were fully rescued by AFD-specific expression of wild-type CMK-1 (Figure 1C-D). In all cases where significant IT behavior was observed, animals tracked isotherms in a temperature range similar to that tracked by wildtype animals (Figure S1). Thus, CMK-1 acts in AFD to mediate both negative thermotaxis and IT behaviors.

We next investigated the neuronal basis for the behavioral defects in *cmk-1* mutants by examining temperature-induced intracellular calcium dynamics in AFD using the genetically encoded YC3.60 calcium sensor (Miyawaki et al., 1997). We measured responses to a rising linear temperature ramp with a superimposed sinusoidal oscillation (Figure 2A, 2D), a stimulus that allows accurate quantification of T^*_{AFD} over background noise (Clark et al., 2006). Both T^*_{AFD} and response amplitude were significantly decreased in *cmk-1(oy21)* mutants (Figure 2A-F), with stronger defects in animals grown overnight at 20°C or 25°C than in animals grown at 15°C (Figure 2A-F, Table S1). T^*_{AFD} and response amplitudes

were fully rescued by AFD-specific expression of --type CMK-1 (Figure 2A-F), indicating that CMK-1 acts cell autonomously to regulate temperature-evoked calcium dynamics in AFD. We conclude that CMK-1 is required to set the correct T^*_{AFD} upon growth at a specific T_c, and that this requirement is particularly critical at warmer temperatures.

While the maximal T^*_{AFD} is lower in *cmk-1* mutants than in wild-type animals grown overnight at a given temperature, T^*_{AFD} nevertheless adapts in *cmk-1* mutants shifted to a new temperature (Figure 2B, 2E, Table S1). Since T^*_{AFD} is correlated with T_c-regulated intracellular cGMP levels (Wang et al., 2013; Wasserman et al., 2011), T^*_{AFD} can be affected by either changes in the rate of cGMP synthesis and/or hydrolysis, or by the magnitude of cGMP concentration change upon growth at different temperatures. We examined this issue by comparing the dynamics of T^*_{AFD} adaptation in wild-type and *cmk-1* mutants in animals shifted between two temperatures for different periods of time. Since T^*_{AFD} defects were most pronounced at 25°C (Table S1), we chose to shift animals between 15°C and 25°C.

To investigate T^*_{AFD} adaptation dynamics in detail, we performed temperature shift experiments at high temporal resolution. Animals were shifted between 15-25°C every 1-5 minutes up to 30 minutes, or for longer time intervals up to 24 hours prior to measuring T^*_{AFD}. In temperature upshift experiments, we found that exposure to 25°C for as little as 1 minute was sufficient to significantly increase T^*_{AFD} in wild-type animals (Figure 2G). The time course of the change in T^*_{AFD} evoked by temperature upshift was best fit by a double exponential function ($P<0.001$). This finding reveals that T^*_{AFD} adaptation involves both a fast and slow process and helps to reconcile disparate findings from electrophysiology (Ramot et al., 2008a) and calcium imaging (Biron et al., 2006) experiments. The initial, rapid phase of T^*_{AFD} adaptation had a time constant of ~2-3 minutes (τ_1, Figure 2G) that matches prior results from electrophysiology (Ramot et al., 2008a), whereas a later, slower phase of adaptation occurred with a time constant of ~3-5 hours ($\tau 2$, Figure 2G) that matches measurements derived from calcium imaging (Biron et al., 2006). Neither the estimated time constants, nor their respective contributions, to the timecourse were significantly altered in *cmk-1* mutants (Figure 2G). [The contribution of the slow and fast components to the overall time course was: WT – 0.48 (slow) and 0.52 (fast); *cmk-1* – 0.48 (slow) and 0.53 (fast)].

Similar experiments for temperature downshift showed that T^*_{AFD} adapted to lower temperatures following a single exponential timecourse with a time constant of ~3 hours (Figure 2H). As in the case of upshifts, *cmk-1* mutants did not exhibit significant defects in the rate of adaptation to lower temperatures (Figure 2H). Based on these observations, we infer that the altered T^*_{AFD} in *cmk-1* mutants upon exposure to a new temperature results from a reduction in the overall magnitude, but not the rate of change in cGMP concentration.

We next investigated the mechanism by which T^*_{AFD} is adapted to a T_c-correlated value and the role of CMK-1 in this process. Previously, we showed that loss of function of one or more of the AFD-specific *gcy-8, gcy-18* and *gcy-23* rGC genes results in lowered T^*_{AFD} at a given T_c (Wasserman et al., 2011), suggesting that these genes contribute to setting the correct T^*_{AFD}. Given that the slow phase of T^*_{AFD} adaptation takes hours, we considered

the possibility that temperature alters expression of the AFD-specific *gcy* genes to regulate intracellular cGMP levels.

Consistent with this hypothesis, we found that *gcy-8*p::GFP fluorescence levels in AFD were correlated with the overnight cultivation temperature (Figure 3A). Additionally, qRT-PCR experiments showed that expression of all three AFD-specific *gcy* genes increased 3-5-fold upon overnight growth at warmer temperatures (Figure 3B). Expression of non-thermosensory genes were not similarly affected by growth temperature (Figure 3B), indicating that the changes in *gcy* gene expression were not due to a non-specific increase in gene expression at warmer temperatures. We also characterized the dynamics of *gcy* gene expression change upon temperature shift by quantifying endogenous *gcy* mRNA levels by qRT-PCR at different timepoints following temperature shift. In temperature upshift and downshift experiments, we observed significant up- or downregulation of *gcy* gene expression, respectively, on different but long timescales (Figures 3C-D).

Since a major mechanism by which CaMK proteins regulate neuronal functions is via activity-dependent regulation of gene expression (Wayman et al., 2008), we asked whether the observed T_c-dependent changes in *gcy* gene expression are mediated by CMK-1. Quantification of *gcy-8*p::GFP fluorescence (Figure 3A, Figure S2A), or of endogenous *gcy* message levels via qRT-PCR (Figure 3B), showed that unlike in wild-type animals, *gcy* gene expression levels were not increased upon warming in *cmk-1(oy21*) mutants, resulting in a stronger expression defect in *cmk-1* mutants relative to wild-type animals at warmer temperatures. *gcy-8*p*::*GFP fluorescence was also decreased in *cmk-1(oy21)* animals grown at 15°C (Figure 3A) (Satterlee et al., 2004), although we could not reliably detect changes in endogenous mRNA levels under these conditions likely due to low expression levels at this temperature (Figure S2B). Both basal and T_c-dependent regulation of *gcy-8*p*::*GFP expression levels was rescued upon expression of wild-type CMK-1 (Figure 3A). Together with previous observations that loss of *gcy* gene function (Wasserman et al., 2011), and growth in 8-Br-cGMP or loss of *pde* phosphodiesterase gene function, lower and raise T^*_{AFD}, respectively (Wang et al., 2013; Wasserman et al., 2011), these results suggest that CMK-1-mediated changes in *gcy* gene expression contribute to long-term T^*_{AFD} adaptation particularly at $T>T_c$.

Mammalian CaMKI/IV is localized either to the cytoplasm or the nucleus based on cellular context and conditions (Wayman et al., 2008). Given the role of CMK-1 in regulating *gcy* gene expression in AFD during adaptation, we asked whether CMK-1 is localized to the nucleus in AFD, and whether its subcellular localization is T_c-dependent. In animals grown overnight at 15°C, functional CMK-1::GFP protein was present at similar levels in both the cytoplasm and the nucleus of AFD (Figure 4A-B). However, upon overnight growth at T_c=25°C, CMK-1::GFP was enriched in the cytoplasm of AFD (Figure 4A-B). In contrast, CMK-1::GFP was enriched in the cytoplasm of the AWC sensory neurons regardless of growth temperatures (Figure S3A).

We investigated the dynamics of CMK-1 subcellular localization by examining CMK-1::GFP in AFD upon temperature up- and downshift between 15°C and 25°C. Exposing animals grown at 15°C overnight to 25°C for 15 minutes was sufficient to enrich

CMK-1::GFP in the AFD nucleus (Figure 4A-B). This localization change was transient, since by 60 minutes after the shift the localization pattern of CMK-1::GFP in AFD was similar to that of animals grown overnight at 25°C (Figure 4A-B). In contrast, upon a temperature downshift from 25°C to 15°C, we observed a gradual and slow change in CMK-1::GFP subcellular localization (Figure 4B). These results indicate that subcellular localization of CMK-1 in AFD is dynamic, particularly upon temperature upshift, and depends on the duration of exposure to a given T_c.

We asked whether constitutive localization of CMK-1 to either the cytoplasm or nucleus affects its ability to regulate AFD function. Addition of a nuclear localization sequence (NLS) or nuclear export sequence (NES) caused GFP-tagged CMK-1 protein to be ~5-fold enriched in the AFD nucleus or cytoplasm, respectively (Figure S3B). The localization of fusion proteins bearing an NLS or NES was not obviously affected during temperature shifts or upon growth at a new T_c (Figure S3B). Both CMK-1+NLS and CMK-1+NES rescued the gene expression and behavioral defects, as well as defects in temperature-induced calcium dynamics in AFD of *cmk-1(oy21)* mutants regardless of growth temperature (Figure S4A-D), although expression of CMK-1+NLS consistently resulted in higher *gcy-8*p*::gfp* expression and T^*_{AFD} values than expression of CMK-1+NES (Figure S4C-D). Although these results can be interpreted to indicate that CMK-1 can function either in the cytoplasm or in the nucleus to regulate overall AFD thermosensory properties, we favor the alternate hypothesis that a fraction of both overexpressed molecules continues to shuttle between the cytoplasm and nucleus upon temperature shift, with increased nuclear localization resulting in higher gene expression and T^*_{AFD} (also see below).

The functions of mammalian CaMKI/IV as well as *C. elegans* CMK-1 *in vitro*, are potentiated via phosphorylation by an upstream CaM-dependent kinase (CaMKK) (Eto et al., 1999; Wayman et al., 2008). We examined thermosensory behaviors of animals lacking *ckk-1* CaMKK to determine whether these animals exhibit behavioral defects similar to those of *cmk-1* mutants. *ckk-1* null mutants exhibited strong defects in negative thermotaxis behavior (Figure S4A), but wild-type IT behavior when grown at 15°C (Figure S4B). T^*_{AFD} was markedly decreased in *ckk-1* mutants at T_c=25°C although to a lesser extent than in *cmk-1* mutants (Figure 4C); T^*_{AFD} in *ckk-1* mutants was unaffected at T_c=15°C (Figure S4C). Consistent with decreased T^*_{AFD} at T_c=25°C but not at T_c=15°C in *ckk-1* mutants, *gcy-8*p::GFP levels in *ckk-1* mutants were decreased upon overnight growth at 25°C but only weakly affected at 15°C (Figure 4D; Figure S3C). These observations suggest that CKK-1 plays a role in setting T^*_{AFD} at T_c=25°C.

Since calcium influx can regulate nuclear localization of CaMKI isoforms in mammalian cells (Wayman et al., 2008), we asked whether the observed defects in *ckk-1* mutants arise due to altered subcellular localization of CMK-1. Indeed, CMK-1::GFP was constitutively enriched in the cytoplasm of AFD in *ckk-1* mutants regardless of T_c, and nuclear enrichment was not observed during temperature shifts (Figure 4E). The T^*_{AFD} adaptation defect of *ckk-1* mutants at T_c=25°C could arise due to decreased catalytic functions or constitutive cytoplasmic localization of CMK-1. We found that overexpression of CMK-1+NLS robustly increased both T^*_{AFD} and *gcy-8*p::GFP expression levels in AFD in *ckk-1* mutants to values higher than those in wild-type animals, (Figure 4C-D); the localization pattern of

CMK-1+NLS::GFP in AFD was unaltered in *ckk-1* mutants regardless of T_c (Figure S3D). In contrast, CMK-1(T179A)::DsRed in which the CKK-1 target residue has been mutated to alanine (Eto et al., 1999), was strongly enriched in the cytoplasm regardless of T_c (Figure S3E), and failed to rescue the T^*_{AFD} defects of *cmk-1(oy21)* mutants (Figure S3F). Together, these observations suggest that CKK-1-mediated phosphorylation regulates temperature-dependent nuclear translocation, but not activity, of CMK-1 in AFD, and support the idea that nuclear localization of CMK-1 upregulates *gcy* gene expression and T^*_{AFD} at warmer temperatures. CKK-1 similarly regulates nuclear localization of CMK-1 in response to noxious heat in the FLP nociceptor neurons in *C. elegans* (Schild et al., 2014).

CaMK proteins regulate activity-dependent changes in gene expression in part via phosphorylation of transcription factors such as CREB and HSF1 (Eto et al., 1999; Holmberg et al., 2001; Sheng et al., 1991; Wayman et al., 2008), and *crh-1* CREB mutants have been reported to exhibit thermotaxis defects and altered thermotransduction in AFD (Nishida et al., 2011). *crh-1* mutants did not exhibit significant defects in either thermotaxis behaviors or temperature-regulated intracellular calcium dynamics in AFD under our assay conditions (Figure S4A-C). Mutations in the *hsf-1* HSF1 gene in *C. elegans* have also been reported to alter AFD functions in response to temperature (Sugi et al., 2011); we found *hsf-1(sy441)* mutants had higher T^*_{AFD} values than wild-type animals at T_c=25°C and thus exhibited a phenotype distinct from that of *cmk-1* mutants (Figure S4C). These observations suggest that CMK-1 is unlikely to mediate temperature-regulated gene expression by simply activating CREB, or HSF-1, in AFD.

DISCUSSION

The AFD neurons retain exquisite sensitivity across the physiological temperature range of *C. elegans*, allowing animals to detect temperature changes of <0.01°C from 15-25°C. The wide dynamic range of AFD is mediated by adaptation of T^*_{AFD}, which determines the lower bound of its operating range. T^*_{AFD} is determined by temperature-regulated changes in the balance between cGMP synthesis by rGCs (Inada et al., 2006; Wasserman et al., 2011) and hydrolysis by phosphodiesterases such as PDE-2 (Wang et al., 2013). Adaptation of T^*_{AFD} to a T_c-correlated value is likely mediated by absolute levels of intracellular cGMP and/or calcium (Wang et al., 2013). Consistent with this hypothesis, T^*_{AFD} is set to a lower value in single *gcy* mutants, but is higher in animals grown in 8-Br-cGMP or in *pde-2* mutants (Wang et al., 2013; Wasserman et al., 2011).

Given its timescale of minutes, the fast phase of warm adaptation likely arises from non-transcriptional mechanisms. Similar to light adaptation in vertebrate photoreceptors (see for example Arshavsky and Burns, 2012), we propose that during the initial stages of warming, increased cGMP and calcium levels feed back via CMK-1 and other molecules to decrease rGC or increase PDE activity, or to increase the threshold of cGMP-gated channel activation resulting in a higher value for T^*_{AFD} (Figure 4F). However, upon prolonged exposure to warmer temperatures, adaptation of T^*_{AFD} to the correct value requires CKK-1-mediated regulation of CMK-1 nuclear localization, and CMK-1-mediated changes in *gcy* and other gene expression to increase intracellular cGMP levels (Figure 4F). Similarly, CMK-1 activity in the cytoplasm or nucleus of the nociceptive FLP neurons also increases or

decreases the behavioral threshold, respectively, for heat nociception in *C. elegans* (Schild et al., 2014). In the absence of CMK-1 function, T^*_{AFD} adapts at the same rate but to lower values due to reduced levels of GCY proteins, thereby narrowing the effective dynamic range of AFD. This failure to correctly adapt T^*_{AFD} results in severe thermotaxis behavioral phenotypes. Although CMK-1 may also play a role in regulating *gcy* gene expression at 15°C, the processes underlying adaptation to warmer and colder temperatures are likely to be partly distinct. Together, our results implicate CMK-1-mediated gene expression changes as a major contributor to long-term adaptation of the response threshold of the AFD thermosensory neurons.

The fast and slow thermal adaptation observed in AFD upon temperature upshift is reminiscent of the extensively described transcription-independent and -dependent temporal phases of neuronal and behavioral plasticity observed in multiple systems (Davis, 2005; Hawkins et al., 2006; Huganir and Nicoll, 2013; Leslie and Nedivi, 2011). A few studies have reported related mechanisms contributing to short- and long-term adaptation of peripheral sensory neuron responses. For instance, long-term adaptation of *C. elegans* to volatile odorants, or of *Drosophila* to an initially aversive tastant, is mediated via experience-dependent changes in sensory rGC gene expression or TRPL cation channel protein levels, respectively, in sensory neurons (Juang et al., 2013; Zhang et al., 2013). Adaptation at the sensory neuron response level may provide a simple mechanism to prevent heterologous adaptation to other cues, and allow cross-modulation of responses to other stimuli sensed by the neuron, whereas adaptation at central loci may allow state-dependent modulation of sensory responses, as well as adaptation to multiple features of complex stimuli. Given the intriguing parallels in sensory transduction mechanisms, as well as the adaptation of sensory neuron responses over a broad range of stimulus intensities on different timescales, we suggest that similar temporally distinct transcription-independent and -dependent mechanisms may contribute to expand the operating range of sensory neurons in multiple systems.

EXPERIMENTAL PROCEDURES

Detailed protocols are listed in Supplemental Experimental Procedures.

Thermotaxis behavioral assays

Negative thermotaxis and isothermal tracking assays were performed as described (Beverly et al., 2011; Wasserman et al., 2011). For negative thermotaxis assays, the gradient excluded the temperature range in which animals track isotherms in order to minimize confounds from IT behavior.

In vivo calcium imaging

Imaging of temperature-evoked calcium responses in AFD neurons was performed essentially as previously described (Wasserman et al., 2011). Individual animals were imaged for 6-10 min with an upward ramp that changed at 0.01°C/sec with superimposed sinusoidal oscillations of 0.2°C amplitude and 0.04 Hz frequency.

qPCR

qRT-PCR experiments were performed using RNA from growth synchronized young adult animals. Expression levels of each gene were normalized to *act-1* RNA levels at each temperature.

Quantification of GFP fluorescence

To control for differences in intrinsic GFP fluorescence at different temperatures, *gcy-8*p*::gfp* levels in AFD were normalized to GFP fluorescence levels in the nonthermosensory PVQ neuron in animals grown at 15°C and 25°C.

Supplementary Material

Refer to Web version on PubMed Central for supplementary material.

Acknowledgements

We thank the Sengupta lab for discussions, M. O'Donnell for help with data analysis, J. Yoon and I. Nechipurenko for experimental assistance, the *Caenorhabditis* Genetics Center for strains, and members of the Sengupta lab and C. Bargmann, L. Griffith and S. Wasserman for comments on the manuscript. This work was supported in part by the NIH (R01 GM081639 and collaborative supplement – P.S. and M.B.G.; P30 NS45713 – Brandeis Biology; R21 NS061147 – M.B.G.; R01 NS047715 – M.B.G.), the NSF (IOS 0725079 – M.B.G.), the Swiss National Science Foundation (PZ00P3_131943 – D.A.G), and the European Commission (PCIG10-GA-2011-302077 – D.A.G.).

REFERENCES

Arshavsky VY, Burns ME. Photoreceptor signaling: supporting vision across a wide range of light intensities. J. Biol. Chem. 2012; 287:1620–1626. [PubMed: 22074925]

Bao M, Engel SA. Distinct mechanism for long-term contrast adaptation. Proc. Natl. Acad. Sci. USA. 2012; 109:5898–5903. [PubMed: 22454502]

Beverly M, Anbil S, Sengupta P. Degeneracy and signaling within a sensory circuit contributes to robustness in thermosensory behaviors in *C. elegans*. 2011; 31:11718–11727.

Clark DA, Biron D, Sengupta P, Samuel ADT. The AFD sensory neurons encode multiple functions underlying thermotactic behavior in *C. elegans*. J. Neurosci. 2006; 26:7444–7451. [PubMed: 16837592]

Dalton P, Wysocki CJ. The nature and duration of adaptation following long-term odor exposure. Percept. Psychophys. 1996; 58:781–792. [PubMed: 8710455]

Davis RL. Olfactory memory formation in *Drosophila*: from molecular to systems neuroscience. Annu. Rev. Neurosci. 2005; 28:275–302. [PubMed: 16022597]

Eto K, Takahashi N, Kimura Y, Masuho Y, Arai K, Muramatsu MA, Tokumitsu H. Ca(2+)/Calmodulin-dependent protein kinase cascade in *Caenorhabditis elegans*. Implication in transcriptional activation. J. Biol. Chem. 1999; 274:22556–22562. [PubMed: 10428833]

Garrity PA, Goodman MB, Samuel AD, Sengupta P. Running hot and cold: behavioral strategies, neural circuits, and the molecular machinery for thermotaxis in *C. elegans* and *Drosophila*. Genes Dev. 2010; 24:2365–2382. [PubMed: 21041406]

Hawkins RD, Kandel ER, Bailey CH. Molecular mechanisms of memory storage in *Aplysia*. Biol. Bull. 2006; 210:174–191. [PubMed: 16801493]

Hedgecock EM, Russell RL. Normal and mutant thermotaxis in the nematode *Caenorhabditis elegans*. Proc. Natl. Acad. Sci. USA. 1975; 72:4061–4065. [PubMed: 1060088]

Holmberg CI, Hietakangas V, Mikhailov A, Rantanen JO, Kallio M, Meinander A, Hellman J, Morrice N, MacKintosh C, Morimoto RI, et al. Phosphorylation of serine 230 promotes inducible transcriptional activity of heat shock factor 1. EMBO J. 2001; 20:3800–3810. [PubMed: 11447121]

Huganir RL, Nicoll RA. AMPARs and synaptic plasticity: the last 25 years. Neuron. 2013; 80:704–717. [PubMed: 24183021]

Inada H, Ito H, Satterlee J, Sengupta P, Matsumoto K, Mori I. Identification of guanylyl cyclases that function in thermosensory neurons of *Caenorhabditis elegans*. Genetics. 2006; 172:2239–2252. [PubMed: 16415369]

Juang BT, Gu C, Starnes L, Palladino F, Goga A, Kennedy S, L'Etoile ND. Endogenous nuclear RNAi mediates behavioral adaptation to odor. Cell. 2013; 154:1010–1022. [PubMed: 23993094]

Jurado P, Kodama E, Tanizawa Y, Mori I. Distinct thermal migration behaviors in response to different thermal gradients in *Caenorhabditis elegans*. Genes Brain Behav. 2010; 9:120–127. [PubMed: 20002199]

Kimura KD, Miyawaki A, Matsumoto K, Mori I. The *C. elegans* thermosensory neuron AFD responds to warming. Curr. Biol. 2004; 14:1291–1295. [PubMed: 15268861]

Kurahashi T, Menini A. Mechanism of odorant adaptation in the olfactory receptor cell. Nature. 1997; 385:725–729. [PubMed: 9034189]

Leslie JH, Nedivi E. Activity-regulated genes as mediators of neural circuit plasticity. Prog. Neurobiol. 2011; 94:223–237. [PubMed: 21601615]

Luo L, Cook N, Venkatachalam V, Martinez-Velazquez LA, Zhang X, Calvo AC, Hawk J, Macinnis BL, Frank M, Ng JH, et al. Bidirectional thermotaxis in *Caenorhabditis elegans* is mediated by distinct sensorimotor strategies driven by the AFD thermosensory neurons. Proc. Natl. Acad. Sci. USA. 2014; 111:2776–2781. [PubMed: 24550307]

Miyawaki A, Llopis J, Heim R, McCaffery JM, Adams JA, Ikura M, Tsien RY. Fluorescent indicators for Ca2+ based on green fluorescent proteins and calmodulin. Nature. 1997; 388:882–887. [PubMed: 9278050]

Mori I, Ohshima Y. Neural regulation of thermotaxis in *Caenorhabditis elegans*. Nature. 1995; 376:344–348. [PubMed: 7630402]

Nishida Y, Sugi T, Nonomura M, Mori I. Identification of the AFD neuron as the site of action of the CREB protein in *Caenorhabditis elegans* thermotaxis. EMBO Rep. 2011; 12:855–862. [PubMed: 21738224]

Patapoutian A, Tate S, Woolf CJ. Transient receptor potential channels: targeting pain at the source. Nat. Rev. Drug Discov. 2009; 8:55–68. [PubMed: 19116627]

Ramot D, MacInnis BL, Goodman MB. Bidirectional temperature-sensing by a single thermosensory neuron in *C. elegans*. Nat. Neurosci. 2008a; 11:908–915. [PubMed: 18660808]

Ramot D, MacInnis BL, Lee HC, Goodman MB. Thermotaxis is a robust mechanism for thermoregulation in *Caenorhabditis elegans* nematodes. J. Neurosci. 2008b; 28:12546–12557. [PubMed: 19020047]

Satterlee JS, Ryu WS, Sengupta P. The CMK-1 CaMKI and the TAX-4 Cyclic nucleotide-gated channel regulate thermosensory neuron gene expression and function in *C. elegans*. Curr. Biol. 2004; 14:62–68. [PubMed: 14711416]

Schild LC, Zbinden L, Bell HW, Yu YV, Sengupta P, M.B. G, Glauser DA. The balance between cytoplasmic and nuclear CaMK Kinase-1 signaling controls the operating range of noxious heat avoidance. Neuron. 2014 this issue.

Sheng M, Thompson MA, Greenberg ME. CREB: a Ca(2+)-regulated transcription factor phosphorylated by calmodulin-dependent kinases. Science. 1991; 252:1427–1430. [PubMed: 1646483]

Sokolov M, Lyubarsky AL, Strissel KJ, Savchenko AB, Govardovskii VI, Pugh EN Jr. Arshavsky VY. Massive light-driven translocation of transducin between the two major compartments of rod cells: a novel mechanism of light adaptation. Neuron. 2002; 34:95–106. [PubMed: 11931744]

Sugi T, Nishida Y, Mori I. Regulation of behavioral plasticity by systemic temperature signaling in *Caenorhabditis elegans*. Nat. Neurosci. 2011; 14:984–992. [PubMed: 21706021]

Wang D, O'Halloran D, Goodman MB. GCY-8, PDE-2, and NCS-1 are critical elements of the cGMP-dependent thermotransduction cascade in the AFD neurons responsible for *C. elegans* thermotaxis. J. Gen. Physiol. 2013; 142:437–449. [PubMed: 24081984]

Wasserman SM, Beverly M, Bell HW, Sengupta P. Regulation of response properties and operating range of the AFD thermosensory neurons by cGMP signaling. Curr. Biol. 2011; 21:353–362. [PubMed: 21315599]

Wayman GA, Lee YS, Tokumitsu H, Silva AJ, Soderling TR. Calmodulin-kinases: modulators of neuronal development and plasticity. Neuron. 2008; 59:914–931. [PubMed: 18817731]

Zhang YV, Raghuwanshi RP, Shen WL, Montell C. Food experience-induced taste desensitization modulated by the *Drosophila* TRPL channel. Nat. Neurosci. 2013; 16:1468–1476. [PubMed: 24013593]

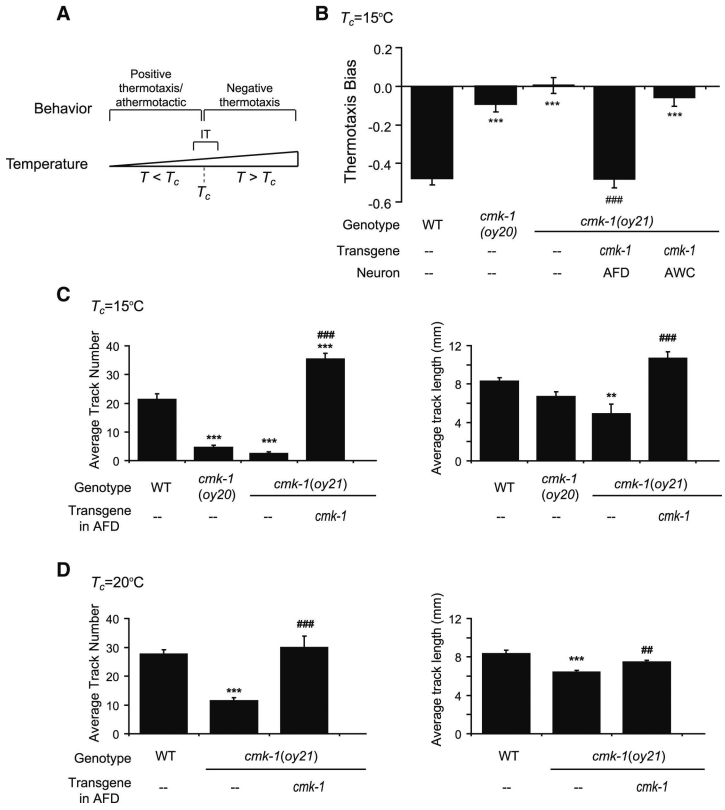

Figure 1.

cmk-1 mutants exhibit defects in negative thermotaxis and isothermal tracking behaviors.

A. Thermotaxis behaviors exhibited at ambient temperatures (*T*) relative to cultivation temperature (T_C). IT – isothermal tracking behavior.

B. Thermotaxis bias of the indicated strains on a spatial thermal gradient. *cmk-1* cDNA was expressed specifically in AFD and AWC under the *ttx-1* and *ceh-36* promoters, respectively. Bars (± SEM) are the average of 10 independent assays of 15 animals each. Wild-type and mutant strains were examined together on multiple days. *** indicates different from wild-type at $P<0.001$; ### indicates different from *cmk-1(oy21)* at $P<0.001$ (ANOVA and Bonferroni post-hoc corrections).

C-D. Average track numbers (left) and lengths (right) of strains grown at the indicated temperatures. Animals grown at 25°C do not track well (Y.Y. and H.B., unpublished observations). Bars (± SEM) are the average of 8-10 independent assays of 15 animals each. Wild-type and mutant strains were examined together on multiple days. ** and *** indicate different from wild-type at $P<0.01$ and 0.001, respectively; ## and ### indicate different from *cmk-1(oy21)* at $P<0.01$ and 0.001, respectively (Kruskal-Wallis nonparametric ANOVA and Bonferroni post-hoc corrections). See Figure S1 for average tracking temperatures.

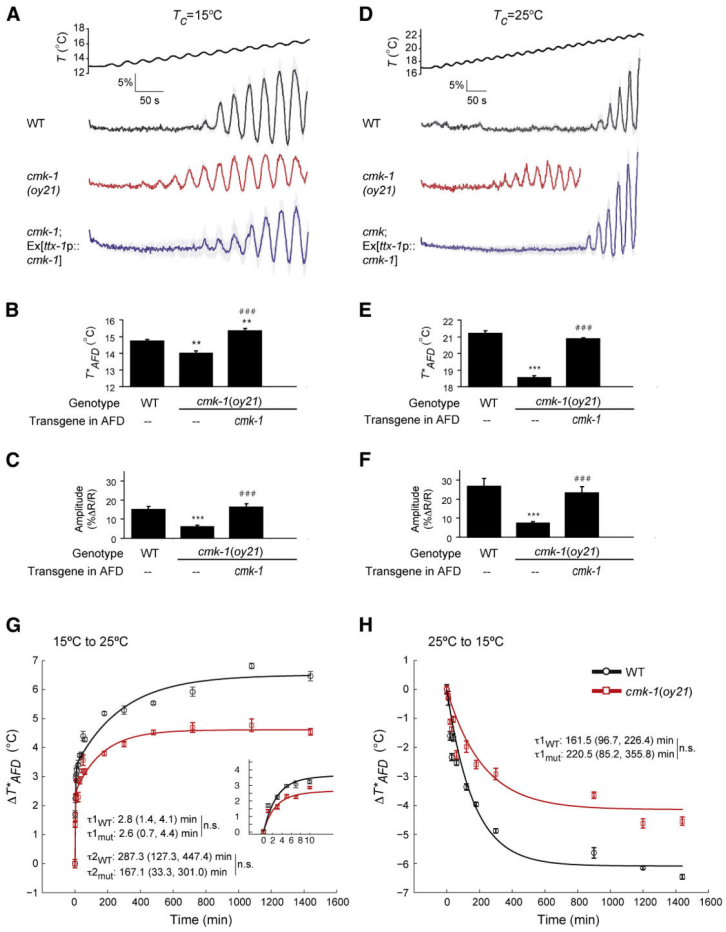

Figure 2.

T^*_{AFD} and AFD thermosensory responses are decreased in *cmk-1* mutants. **A-F.** Average calcium responses in AFD evoked by a rising temperature stimulus. Since all animals were imaged for the same period of time, imaging of *cmk-1(oy21)* animals grown at 25°C was terminated at a lower temperature. Error bars are SEM. n≥9 neurons each. (**B, E**) Average T^*_{AFD} and (**C, F)** average response amplitudes (see Supplemental Experimental Procedures) in the indicated strains. ** and *** indicate different from wild-type values at $P<0.01$ and 0.001, respectively; ### indicates different from *cmk-1(oy21)* at $P<0.001$ (ANOVA and Bonferroni post-hoc corrections). Also see Table S1 for average T^*_{AFD} at different growth temperatures.

G-H. Dynamics of T^*_{AFD} adaptation in wild-type and *cmk-1(oy21)* animals during temperature shift over 24 hours or the initial 10 minutes (**G** inset). Black and red lines are exponential fits to the data for wild-type and *cmk-1(oy21)* mutants, respectively. Time constants (±95% confidence interval) are indicated. n.s. – not significantly different between indicated values. WT – wildtype, mut – *cmk-1(oy21)*. Strains were examined together on multiple days. Each point is the average of 5-10 AFD neurons; error bars are SEM.

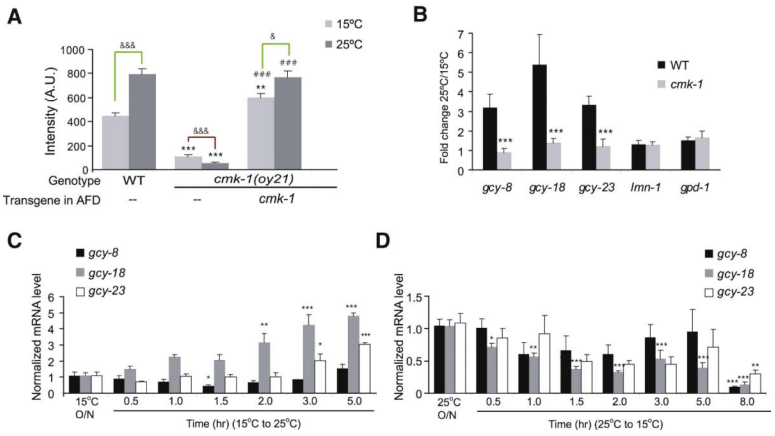

Figure 3.

Expression of AFD-expressed *gcy* genes is altered in a CMK-1-dependent manner upon prolonged growth at specific temperatures.

A. GFP fluorescence levels in AFD of a stably integrated *gcy-8*p*::gfp* reporter gene as a function of T_c and genetic background. See Figure S2A for expression levels at T_c=20°C. Bars (± SEM) are the average of n>15 neurons for each condition. ** and *** indicate different from corresponding wild-type values at P<0.01 and 0.001, respectively; ### indicates different from corresponding *cmk-1(oy21)* values at P<0.001; & and &&& indicate different between indicated values (green brackets - upregulated at 25°C, red brackets – downregulated at 25°C) at P<0.05 and 0.001, respectively (ANOVA and Bonferroni post-hoc corrections).

B. Fold-change in mRNA levels of *gcy*, *lmn-1* lamin or *gpd-1* GAPDH genes as a function of T_c in wild-type or *cmk-1(oy21)* animals. Bars (± SEM) are averages of 3-4 independent biological replicates, each analyzed in triplicate. *** indicate different from wild-type at P<0.001 (ANOVA and Bonferroni post-hoc corrections). See Figure S2B for quantification of mRNA levels in wild-type or *cmk-1* mutants grown at 15°C.

C-D. Fold-change in mRNA levels of *gcy-8*, *gcy-18* and *gcy-23* in wild-type animals at the indicated times following temperature shift. Bars (± SEM) are the averages of 3-4 independent biological replicates, each analyzed in triplicate. *, ** and *** indicate different from corresponding initial values at P<0.05, 0.01 and 0.001, respectively (ANOVA and Bonferroni post-hoc corrections).

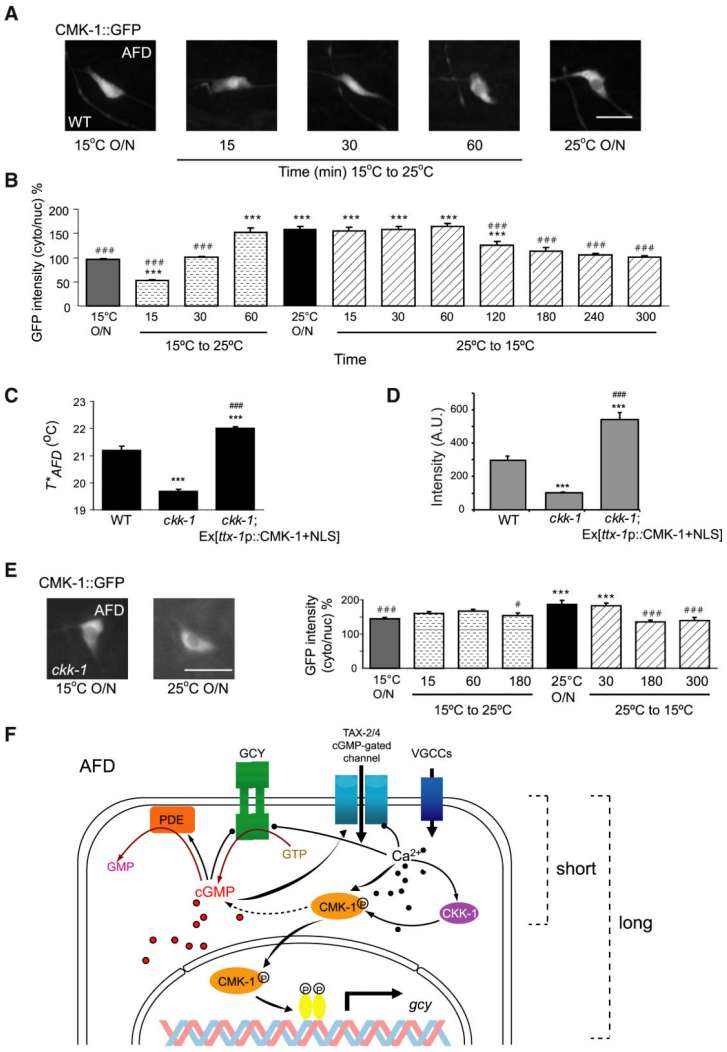

Figure 4.

The subcellular localization of CMK-1 in AFD is regulated by temperature and CKK-1 CaMKK.

A. Representative images of subcellular localization of a functional CMK-1::GFP protein in AFD in wild-type animals grown at the indicated temperatures or upon temperature shift. Scale bar – 10 μm.

B. The ratio of fluorescence levels of *ttx-1* promoter-driven CMK-1::GFP in the cytoplasm and the nucleus of AFD in *cmk-1(oy21)* animals at the indicated growth temperatures or upon temperature shift for the shown time periods. Bars (± SEM) are averages of results from n>15 animals analyzed in 2-3 independent experiments. *** and ### indicate different from values upon overnight growth at 15°C and 25°C, respectively at $P<0.001$ (ANOVA and Bonferroni post-hoc corrections). See Figures S3 and S4 for quantification of subcellular localization, behavior, gene expression, and T^*_{AFD} phenotypes of animals expressing CMK-1+NLS and CMK-1+NES in AFD. **C.** Average T^*_{AFD} of animals of the indicated genotypes grown at 25°C. The *ckk-1(ok1033)* allele was used. *** and ### indicate different from wild-type and *cmk-1* values, respectively at $P<0.001$ (ANOVA and

Bonferroni post-hoc corrections). Bars (±SEM) are averages from n=8-9 neurons. See Figures S3D for subcellular localization of CMK-1+NLS::GFP in AFD in *ckk-1* mutants.
D. GFP fluorescence levels in AFD of a stably integrated *gcy-8*p*::gfp* reporter gene. Bars (±SEM) are averages from n>14 neurons for each condition. *** indicates different from corresponding wild-type values at $P<0.001$; ### indicates different from corresponding *ckk-1(ok1033)* values at $P< 0.001$ (ANOVA and Bonferroni post-hoc corrections).
E. Representative images (left) and quantification (right) of *ttx-1* promoter-driven CMK-1::GFP localization in AFD in *ckk-1(ok1033)* mutants. Bars (± SEM) are the average of n>13 animals analyzed in 2 independent experiments. *** indicates different from values upon overnight growth at 15°C at $P<0.001$; # and ### indicate different from values upon overnight growth at 25°C at $P<0.05$ and 0.001, respectively (ANOVA and Bonferroni post-hoc corrections). Scale bar – 10 μm.
F. Working model of molecular mechanisms underlying short- and long-term adaptation of T^*_{AFD} to T_c upon temperature upshift. VGCC – voltage-gated calcium channel. See Discussion for details.